The Brain Circuitry Underlying the Temporal Evolution of Nausea in Humans

Vitaly Napadow[1,2], James D. Sheehan[3], Jieun Kim[1,2], Lauren T. LaCount[1,2], Kyungmo Park[4], Ted J. Kaptchuk[5], Bruce R. Rosen[1,2] and Braden Kuo[3]

[1]Martinos Center for Biomedical Imaging, Charlestown, MA 02129, USA, [2]Department of Radiology, Massachusetts General Hospital, Charlestown, MA, USA, [3]Gastroenterology Unit, Massachusetts General Hospital, Harvard Medical School, Boston, MA, USA, [4]Department of Biomedical Engineering, Kyunghee University, Yongin, Republic of Korea and [5]Beth Israel Deaconess Medical Center, Harvard Medical School, Boston, MA, USA

Address correspondence to Vitaly Napadow, PhD, Martinos Center for Biomedical Imaging, 149 Thirteenth Street #2301, Charlestown, MA 02129, USA. Email: vitaly@nmr.mgh.harvard.edu.

Nausea is a universal human experience. It evolves slowly over time, and brain mechanisms underlying this evolution are not well understood. Our functional magnetic resonance imaging (fMRI) approach evaluated brain activity contributing to and arising from increasing motion sickness. Subjects rated transitions to increasing nausea, produced by visually induced vection within the fMRI environment. We evaluated parametrically increasing brain activity 1) precipitating increasing nausea and 2) following transition to stronger nausea. All subjects demonstrated visual stimulus–associated activation ($P < 0.01$) in primary and extrastriate visual cortices. In subjects experiencing motion sickness, increasing phasic activity preceding nausea was found in amygdala, putamen, and dorsal pons/locus ceruleus. Increasing sustained response following increased nausea was found in a broader network including insular, anterior cingulate, orbitofrontal, somatosensory and prefrontal cortices. Moreover, sustained anterior insula activation to strong nausea was correlated with midcingulate activation ($r = 0.87$), suggesting a closer linkage between these specific regions within the brain circuitry subserving nausea perception. Thus, while phasic activation in fear conditioning and noradrenergic brainstem regions precipitates transition to strong nausea, sustained activation following this transition occurs in a broader interoceptive, limbic, somatosensory, and cognitive network, reflecting the multiple dimensions of this aversive commonly occurring symptom.

Keywords: brain-gut interactions, interoception, motion sickness, neuroimaging

Introduction

Nausea is a subjective experience of unease and a commonly occurring aversive symptom with broad etiology including drug side effects (e.g., postoperative and postchemotherapy nausea) and disease comorbidity. In the clinic, it is typified by epigastric discomfort with the urge to vomit (Quigley et al. 2001). Nausea sensation encompasses stomach awareness, as well as strong emotional and cognitive components (Muth et al. 1996). Given the importance of nausea symptomatology to so many medical fields, it is surprising how little is known about the neurobiology and brain activity underlying this subjective sensation (Kowalski et al. 2006). Thus, a better characterization of the central pattern generator for nausea will lead to better understanding of its neurophysiology, provide brain targets for potential therapies, and more broadly inform the design process for development of "cleaner" drugs, which retain

therapeutic efficacy, but lack nausea and vomiting as side effects (Horn 2008).

Animal studies have implicated brainstem (Stern et al. 2011) and vestibulocerebellum (flocculus and vermis) nuclei, as well as the amygdala (Horn et al. 2007) in the development of emesis. However, difficulties remain in evaluating perception and temporal evolution of emetic precursor symptoms, such as nausea, in animal models. As nausea is typified by epigastric discomfort, additional candidate brain regions for processing nausea in humans would include those associated with interoception. Interoception classically refers to conscious awareness of visceral afference (Dworkin 2007); however, recent theories have expanded this definition to include conscious awareness of internal body state (Craig 2002). Interoceptive afference is thought to project to insula and dorsal anterior cingulate (dACC) cortices (Craig 2002; Critchley et al. 2004; Wiens 2005), and recent studies have demonstrated that interoception may play an important role in emotion (Wiens 2005) and emotional disgust related to nausea (Harrison et al. 2010).

A well established human model for nausea involves motion sickness induced by spinning optokinetic drums (Stern et al. 2011), and it remains to be seen if the neural circuitry subserving interoception and emotion is also activated by motion sickness-induced nausea. While positron emission tomography has been applied to investigate the neural correlates of vection and visual/vestibular sensory mismatch (Brandt et al. 1998), such studies have typically limited exposure duration to avoid motion sickness. Thus, there is great need to better understand how brain activity precipitates and modulates the natural temporal evolution of motion sickness-induced nausea. Specifically, while nausea generally evolves slowly over time, a characteristic likely to be reflected by relatively slow changing brain activity modulations, it is also accompanied by phasic "flushes" of sensation and autonomic outflow to various organs. For instance, phasic peaks of high-frequency heart rate variability (HF-HRV, a marker of cardio-vagal modulation) have been noted just prior to nausea report (Morrow et al. 2000; Lacount et al. 2011). The brain circuitry underlying these phasic and sustained aspects of the nausea experience is currently unknown.

We have applied functional magnetic resonance imaging (fMRI), in conjunction with a custom-built head coil, which allowed subjects to experience visually induced circular vection, leading to nausea. We hypothesized that activation in subcortical and pontine brain regions associated with fear conditioning precipitate transitions to stronger nausea. We further hypothesized that salience and interoceptive processing brain regions,

specifically the anterior insula, demonstrate sustained activation following transitions to stronger nausea.

Materials and Methods

Subjects

Right-handed (Edinburgh Inventory, Oldfield 1971) female subjects were recruited through advertisement and prescreened for susceptibility to motion sickness (motion sickness susceptibility questionnaire, MSSQ, Golding 1998). Subjects experienced a mock MRI behavioral session that included exposure to the nauseogenic stimulus. The subsequent fMRI session occurred at least one week after this behavioral session. fMRI data from twenty-eight (28) subjects (age: 27.3 ± 7.5 years, μ ± σ, range: 21–49) were included in our analysis. An additional 4 subjects' data could not be used due to excessive motion artifact (>3 mm translation on any axis and/or spiking >1.5 mm), MRI coil error, or scanner anxiety.

Prior to both mock and real fMRI evaluation, subjects were instructed to abstain from food and water for 12 h and from cigarettes and alcohol for 24 h. This was deemed necessary for safety reasons, as subjects would be stimulated to the verge of vomiting. All experiments took place between 7 AM and 12 PM at the Martinos Center for Biomedical Imaging in Boston, MA. Informed consent was obtained from all participants, and the protocol was approved by the Human Research Committee of Massachusetts General Hospital.

Experimental Protocol

Subjects were placed, supine, in a 1.5-T Siemens Avanto MRI Scanner (Siemens Medical Systems, Erlangen, Germany). A specialized 23-channel head coil constructed at the Martinos Center for Biomedical Imaging (Wiggins et al. 2006) was used to allow for unimpeded visual stimulation with a field-of-view approximately 150° (Fig. 1A,B). This large unimpeded field of view is critical for inducing motion sickness with visual stimuli (Kowalski et al. 2006). A concave screen was positioned 10 cm in front of their eyes, onto which visual stimuli were projected, from behind.

After a 5-min baseline visual fixation on a black cross, the visual stripes stimulus (see below) was presented and continued until either 1) the subject rated a nausea intensity of 4 or 2) 20 min had expired. The stimulus was then terminated, and subjects were presented with another 5 min of fixation (Fig. 1C). Subjects were instructed to remain as still as possible, focus directly on the stimulus, and maintain a constant rate of breathing to prevent significant intersubject variability in respiratory countermeasures to increasing nausea (Yen Pik Sang et al. 2003). Subjects were asked to keep their eyes open and just let the nausea sensation evolve, knowing that a rating of severe nausea (see below) would terminate the stimulus.

The nauseogenic stimulus was a standardized visual presentation of alternating black (1.2 cm, 6.9° viewing angle) and white (1.85 cm, 10.6° viewing angle) stripes with left-to-right circular motion at 62.5°/s. This left-to-right horizontal translation induces a circular vection sensation wherein subjects experience a false sensation of translating to the left. Such stimulation simulates the visual input provided by a rotating optokinetic drum, commonly used to induce vection (illusory self-motion) and nausea (Koch 1999; Kennedy et al. 2010).

In order to link fMRI data analyses with nausea intensity, subjects used a button box to freely rate (not cued) their overall nausea level ranging from "0" to "4." Subjects practiced rating during the behavioral session and were instructed that a rating of "0" indicated no nausea, "1" indicated "mild" nausea, "2" "moderate" nausea, "3" "strong" nausea, and "4" indicated "severe" nausea approaching the urge to vomit from previous experience and at which point the visual stripes stimulus would be terminated.

Following the experiment, subjects completed the simulator sickness questionnaire (SSQ) (Kennedy et al. 1993), to report the severity of different motion sickness symptoms at each global (0–4) nausea level. As we were specifically interested in the interoceptive aspects of nausea, we calculated the peak stomach awareness score for each subject. We then correlated both peak global nausea level and peak stomach awareness
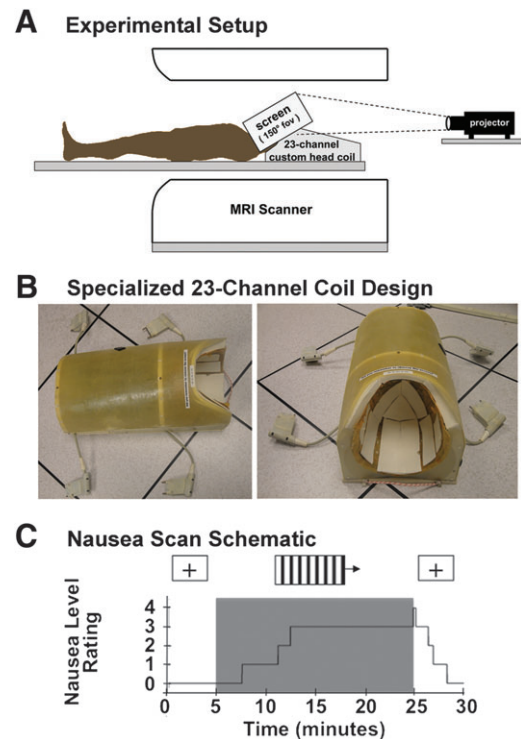

Figure 1. Experimental setup and design. (A) Subjects lay supine inside the MRI scanner while visual stimuli were projected onto a screen encompassing their entire field of view. (B) This setup was made possible with a specially designed, open-configuration multichannel head coil. (C) The fMRI scan run consisted of a visual fixation baseline for 5 min, followed by a visual presentation of alternating black/white stripes translating to the subjects' right field of view (gray background). Over time vection sensation produced nausea, which was rated using a button box (rating shown for a single representative subject). Once subjects rated a nausea level 4 (severe nausea), the stripes stimulation was terminated and subjects fixated again for 5 min.

with subjects' motion sickness susceptibility (MSSQ scores). A nonparametric Spearman rho was calculated using SPSS software (PASW Statistics 18.0, IBM, Armonk, NY), significant at $P < 0.01$.

MRI Scanning Protocol and fMRI Data Analysis

fMRI data were collected using whole-brain blood oxygen level–dependent (BOLD) functional imaging with a gradient echo T_2^*-weighted pulse sequence (time repetition [TR]/time echo [TE] = 3 s/30 ms, slice thickness = 3.6 mm). High-resolution T_1-weighted structural imaging was completed with a standard magnetization prepared rapid gradient echo pulse sequence.

BOLD images were preprocessed using the FMRIB Software Library to correct for magnetic field inhomogeneities, skull stripping, motion correction, and spatial smoothing (full-width at half-maximum = 5 mm). As runtime was lengthy, our data were especially sensitive to motion artifact, which needed to be carefully removed before further analysis. Any residual motion after the steps above was corrected by performing probabilistic independent component analysis and removing components related to motion artifact (e.g., positive/negative fMRI response on opposing edges of the brain, Independent Component time series spikes consistent with prior motion correction time series spikes) (Beckmann and Smith 2004).

fMRI data were analyzed with 2 approaches. In a stimulus-based approach, the entire data run was entered into a subject level general linear model (GLM) with a regressor of interest corresponding to visual stripes stimulation ("off" during crosshair fixation and "on" during horizontal stripes translation, Fig. 2A). Linear drifts were removed via high pass filtering ($t = 128$ s). This approach focused on brain response to visual stimulation with translating stripes. Data were cluster corrected for multiple comparisons using Gaussian random field theory and significant at $P < 0.01$.

A Visual Stimulus fMRI Design

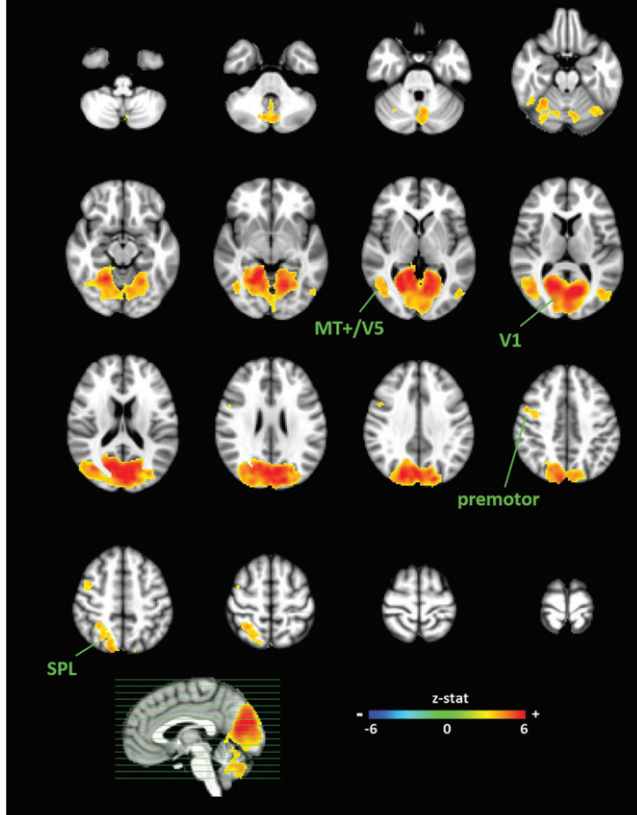## B Brain response to stripes stimulus

Figure 2. Brain fMRI response to visual stimulation with translating stripes. (A) The single block stimulus design contrast brain response to translating stripes with crosshair fixation. (B) Robust fMRI activation was found in primary (V1) and secondary (MT+/V5) visual and visual motion brain areas. Activation was also noted in SPL and premotor areas, as well as cerebellum.

In a percept-based approach, functional data from subjects were analyzed relative to subjects' nausea ratings. Significant nausea was experienced by 19 of the 28 subjects in this analysis. fMRI data were split into 1-min data sets with the temporal midpoint corresponding to nausea transition report (30 s before rating/30 s after) for each transition rating. The 3-to-4 transition was not included since rating a level "4" signaled a transition of the visual stimulus from translating stripes to a simple crosshair (i.e., stimulus offset), thus introducing a new stimulus change not related to nausea sensation increase. Each 1-min data set was high pass filtered ($t = 120$ s) and entered into a subject level GLM with 3 regressors: 1) a 30 s off/30 s on regressor (data from both behavioral and fMRI sessions indicated at least 30 s of stable nausea intensity once a higher level had been achieved); 2) a "phasic" event regressor set at 2 TR's prior to the button press (see below), and 3) a midwindow centered 1 TR event regressor corresponding to the button press and controlling for the motor activity of rating.

The sustained regressor evaluated any persisting change in brain activity once higher nausea intensity was reached—that is, fMRI signal during the higher nausea state was contrast with brain activity in the lower nausea state. The phasic regressor was used to investigate any brain activity that precipitated subsequent rating change. We offset this event regressor by 2 TR's (6 s) from the actual rating transition, as autonomic data from the same subjects demonstrated phasic bursts of HF-HRV (cardiovagal modulation) 6–10 s preceding the button press (Lacount et al. 2011). These phasic bursts may be associated with the autonomic flushes commonly experienced in conjunction with nausea, prompting subjects to rate higher nausea levels.

The resultant parameter estimates were then spatially normalized to Montreal Neurological Institute (MNI) space using anatomical data and the FMRIB Nonlinear Image Registration Tool (FNIRT) (Andersson et al. 2007). These spatially normalized parameter estimates were passed up, with their variances, to higher-level analyses using a mixed-effects model (FLAME, FEAT, FSL) (Beckmann et al. 2003).

Group analyses evaluated increasing brain response with increasing nausea intensity by applying a (−1, 0, 1) contrast. This parametric approach should more specifically reflect nausea perception as it evaluates increasing brain activity with increasing nausea. A group map for the button press event regressor was also calculated as a control. All group maps were corrected for multiple comparisons at a corrected cluster threshold of $P < 0.01$. In addition to this whole-brain analysis, we also performed a region-of-interest (ROI) analysis, with a direct search restricted to the brainstem and cerebellum—regions implicated in previous animal studies of nausea or motion sickness (Stern et al. 2011). The results of this ROI analysis were evaluated using an uncorrected threshold of $z = 3.29$ (two-tailed $P < 0.001$) and a minimum cluster size of 50 mm^3. We also explored variability in brain response to strong nausea transition by calculating the correlation matrix between phasic and sustained response regions. As this correlation matrix included many different tests, all correlations were Bonferroni corrected for multiple comparisons and significant at corrected $P < 0.05$.

In order to estimate the temporal evolution of neuronal activity within the 1-min time windows used in the percept-based analysis, we also calculated a "relative neuronal response" by deconvolving the group-averaged fMRI time series with the double-Gaussian hemodynamic response function used to form our regressors in the fMRI GLM (3dTfitter, AFNI, Cox 1996). This allowed us to analyze estimated neuronal activity in the brain relative to the window-centered button press event.

Results

Our subject cohort reported a broad range of nausea intensities. Eleven (11) subjects ultimately rated a "4" during the course of the experiment. Nineteen (19) subjects rated at least moderate nausea (2 of 4) and contributed fMRI data to the percept-based parametric analysis. The average stimulus duration for subjects who reached rating "4" (and therefore terminated the stimulus before the maximum 20 min) was 9.0 ± 4.7 min ($\mu \pm \sigma$). Importantly, while severe nausea was reached by 11 subjects, no subject vomited or retched during or after nausea induction. In regard to specific sensations, "stomach awareness" reached moderate to severe levels for a global nausea level 3 (level 0: 0.3 ± 0.6, $\mu \pm \sigma$; level 1: 0.8 ± 0.7; level 2: 1.3 ± 0.7; level 3: 2.1 ± 0.6; level 4: 2.5 ± 0.6). Notably, stomach awareness demonstrated significantly increased intensity for each transition evaluated with fMRI data (0 vs. 1: $P = 0.012$; 1 vs. 2: $P = 0.007$; and 2 vs. 3: $P < 0.001$).

A broad range of motion sickness susceptibility was also found in our subject cohort. MSSQ score ranged from nil to 236. MSSQ score was significantly correlated with maximum nausea intensity reached during stimulation (Spearman's rho = 0.82, $P < 0.001$), as well as peak stomach awareness (Spearman's rho = 0.78, $P < 0.001$).

Brain response to translating stripes stimulation was indeed found in regions known to process moving visual stimuli,

including primary visual cortex (V1) and extrastriate areas consistent with MT+/V5 (Fig. 2, Table 1). Activation was also noted in premotor area, superior parietal lobule (SPL), and cerebellum.

Increasing nausea sensation was associated with increasing phasic brain activity prior to rating change in a cluster including the left amygdala and ventral putamen, as well as a dorsal pontine brainstem region consistent with putative locus ceruleus (LC) (Fig. 3, Table 1). No brain areas demonstrated decreasing phasic activity with increasing nausea perception.

Increasing nausea was also associated with increasing sustained brain activity following transition to higher nausea intensity in multiple brain areas (Fig. 4, Table 1). These regions included right frontoinsular (FIC, including the anterior insula), middle/posterior insula, anterior middle cingulate (aMCC/dACC), and both secondary (SII) and primary (SI) somatosensory cortices. The latter was in the SI representation subregion associated with upper gastrointestinal (GI) structures (Coen et al. 2007; Van Oudenhove et al. 2008). Increasing activity was also found in orbitofrontal (OFC), pregenual anterior cingulate (pgACC), dorsolateral prefrontal (dlPFC) and premotor cortices. Subcortical response was noted in putamen, nucleus accumbens (NAcc), and ventral tegmental area (VTA). No brain areas demonstrated decreasing sustained activity with increasing nausea perception. In addition, we calculated a correlation matrix for percent signal change between all brain areas demonstrating significant sustained and phasic response to the transition to strong nausea. The only significant correlation was found between sustained response in the anterior insula and sustained response in the midcingulate cortex ($r = 0.87$, corrected $P = 0.01$, Fig. 5). Thus, subjects who demonstrated greater activation in the anterior insula also demonstrated greater activation in midcingulate cortex. Trending correlations

were also found between the midinsula and both dlPFC ($r = 0.80$, corrected $P = 0.10$) and premotor ($r = 0.81$, corrected $P = 0.07$) cortices.

We also plotted and evaluated relative neuronal activity (created by deconvolution of the fMRI timecourse) within the window used for our percept-based fMRI analyses—that is, centered on the increasing nausea rating transition (Fig. 6). These plots confirmed our interpretation that phasic activation in the amygdala preceded the transition to strong nausea, which was then followed by sustained activation in regions such as the FIC. The timing of these responses was clearly different from the relative neuronal activity timecourse within the contralateral primary motor cortex, M1 (MNI [x, y, z] = –40, –22, 50 mm), which was robustly activated in response to the button press event.

Discussion

Nausea is a commonly experienced aversive state whose central pattern generator is not well understood. Our study applied fMRI to investigate the brain regions subserving different aspects of the temporal evolution of nausea. Increasing nausea sensation was associated with increasing phasic brain response preceding rating transitions in brain

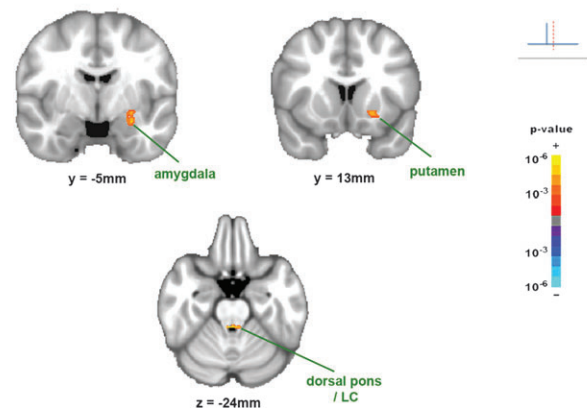### Increasing phasic response preceding nausea rating change

Figure 3. Phasic brain activation preceding nausea rating increase. Increasing response was found in amygdala, ventral putamen, and dorsal pons/LC, suggesting an important role for stress processing and fear conditioning in subjects' decision to rate higher nausea intensity. n.b. amyg = amygdala, put = putamen.

Increasing sustained response with increasing nausea
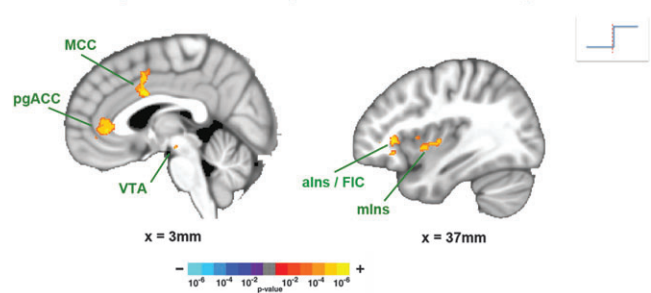

Figure 4. Sustained brain response following nausea rating increase. Increasing sustained response was found in a broad network that included interoceptive (aIns and FIC, aMCC) and emotional (pgACC) brain regions. n.b., aMCC = anterior middle cingulate cortex.

Table 1

Summary of brain regions responding to the visual stimulus as well as those associated with the phasic and sustained response to increasing nausea

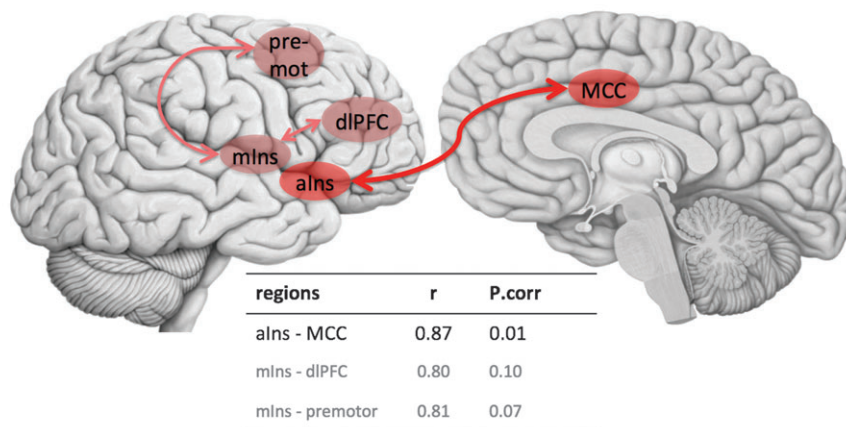|	Side	Cluster size (mm³)	Location (MNI)			Z-score
			x	y	z	
Brain response to translating stripes visual stimulation						
V1	R	143 752	18	−64	6	6.31
	L	143 752	−16	−68	8	6.10
MT+/V5	R	143 752	36	−72	18	5.20
	L	143 752	−42	−70	10	4.26
SPL	R	143 752	30	−50	56	4.66
Premotor	R	2600	50	2	42	4.15
Cerebellar vermis	L	143 752	−6	−64	−30	4.62
Increasing sustained activity following increasing nausea						
anterior insula/FIC	R	8128	40	32	6	4.31
Mid/postinsula	R	8128	36	−8	2	3.63
pgACC	R	4984	10	42	0	4.31
MCC	R	2168	4	8	30	4.61
Putamen	L	5512	−24	12	−8	4.01
NAcc	L	5512	−14	6	−2	3.48
Premotor	R	4440	50	6	32	3.07
OFC	R	8128	30	38	−6	3.86
vmPFC	L	4984	−4	46	−18	3.37
dlPFC	R	8128	46	50	10	3.26
	L	1936	−40	40	18	4.21
SII	R	4440	60	−10	20	4.63
SI	R	4440	48	−14	38	3.52
STG	R	8128	48	10	−8	4.59
VTA	—	232	0	18	−14	4.03
Increasing phasic activity preceding increasing nausea						
Amygdala	L	2120	−28	−4	−16	4.63
Putamen	L	2120	−22	12	−8	3.76
Dorsal pons/LC	L	96	−6	−38	−24	3.94

Figure 5. The correlation matrix connecting our significant phasic and sustained response regions for the transition to strong nausea demonstrated that the only significant correlation ($r = 0.87$, corrected $P = 0.01$) was between sustained response in the anterior insula and midcingulate cortex. Trending (0.05–0.1) correlations were also found between the midinsula cortex and both dlPFC and premotor cortices.

regions known to process stress, emotion, and fear conditioning. Furthermore, once higher nausea intensity was achieved, sustained activation was noted in a broader network of interoceptive, limbic, somatosensory, and cognitive processing brain areas. A correlation analysis demonstrated that subjects who showed greater anterior insula activation following transition to strong nausea also demonstrated greater activation in midcingulate cortex, suggesting a closer linkage between these specific regions within the brain circuitry supporting nausea perception. These results are consistent with the characterization of nausea as a multidimensional perceptual state crossing interoceptive, emotional, and cognitive domains. Our results from a human model of nausea contribute to the growing body of evidence using animal models, supporting limbic and subcortical brain mechanisms for nausea and emesis.
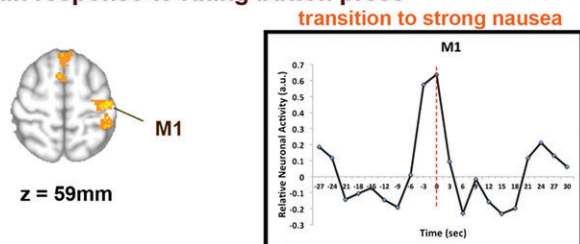
In our study, strong nausea was preceded by phasic activation in the amygdala and putamen, as well as a dorsal pontine brainstem region consistent with the LC. Phasic activity prior to rating change may be related to cardiovagal bursts (HF-HRV) associated with the autonomic flushes that can precede nausea report, evidenced by both our group (Lacount et al. 2011) and similar studies of chemotherapy-induced nausea (Morrow et al. 2000). It is known that visceral signaling provides a powerful interoceptive-conditioning stimulus (Cameron 2001). In our study, subjects' susceptibility to nausea was significantly correlated with peak stomach awareness sensation on the SSQ. Interoceptive conditioning is slower to form, but once established, is more resistant to extinction (Cameron 2001). In fact, this resistance may help maintain the important role of nausea in the conditioned avoidance response in the body's defense against food poisoning. Subjects who experienced nausea in our study tended to report increased susceptibility to motion sickness by the MSSQ and likely a strong conditioned response to nauseogenic stimulation. We suggest that transitions to strong nausea, marked by increased interoception (e.g., stomach awareness), may have provided an aversive fear-conditioning stimulus reflected in phasic activation of the amygdala, LC, and putamen. The amygdala plays a key role in fear processing and conditioning (Ledoux 2003), with input signaling arriving at the lateral nucleus—the most likely localization in our data as well.

Electrophysiological stimulation of the amygdala in monkeys has been reported to produce the appearance of nausea and vomiting (Robinson and Mishkin 1968). The amygdala is also strongly connected with the LC (Valentino et al. 1998), which is the principal source of noradrenergic input to the brain and is strongly associated with a cognitive an emotional stress response (Benarroch 2009). The putamen is involved in procedural memory and repetitive, habitual motor patterns (Graybiel 2005). N-methyl-D-aspartate receptor-mediated activity in the putamen has also been associated with fear conditioning (Schenberg et al. 2006), and, thus, the putamen may work in concert with the amygdala to provide an emotional trigger for subjects to increase their rating to strong nausea.
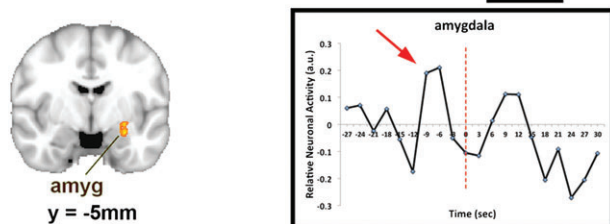
Increasing sustained brain activity with increasing nausea was noted in a broad brain network encompassing multiple domains, including known interoceptive brain regions. Interoception, in its broadest definition, refers to conscious awareness of the physiological state of the body, with interoceptive afference relayed to insula and cingulate cortex via parallel pathways (Craig 2002). Neuroimaging studies of GI sensation (inflated balloon distention) have mapped out visceral interoceptive circuits, and a recent review found most consistent activation in anterior and posterior insula, as well as midcingulate cortex (Mayer et al. 2009). However, visceral balloon inflation stimuli typically produce pain and not nausea. Thus, while interoception from the esophagus and stomach likely play an important role in the perception of nausea, such afference may be necessary but is not sufficient to produce nausea. Our subjects reported interoceptive sensations such as stomach awareness, and fMRI results demonstrated increasing sustained activity in the insula and midcingulate cortex.

Furthermore, a correlation analysis across all brain regions specifically found that subjects who showed greater anterior insula activation following transition to strong nausea also demonstrated greater activation in midcingulate cortex, suggesting a closer linkage between these specific regions—a result quite consistent with previous reports from affective and nonnausea-specific neuroimaging studies (Medford and Critchley 2010). In fact, previous studies have reported that higher-level stimuli (e.g., visual scenes of vomiting) could induce emotional disgust and nausea linked with anterior insula

A. Brain response to rating button press

transition to strong nausea

z = 59mm

M1

B. Phasic brain response preceding rating

amyg

y = -5mm

amygdala

C. Sustained brain response following rating

aIns / FIC
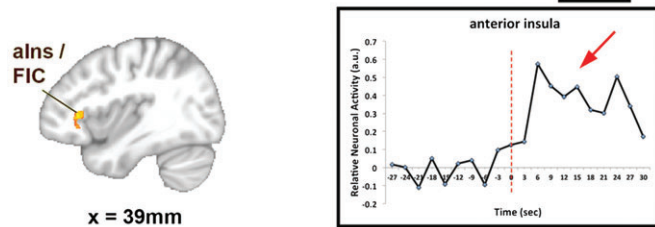
x = 39mm

anterior insula

Figure 6. Time series of brain response. Analysis of group-averaged relative neuronal response (estimated by deconvolution of fMRI time series with the hemodynamic response function) differentiated brain response to increasing nausea from potential confounds such as (A) the motor response underlying the button press event. (B) Increasing phasic response with increasing nausea was seen in the amygdala, where phasic activity preceded the rating change to strong nausea by 6–9 s (red arrow). (C) Increasing sustained response was manifest in anterior insula by persistent brain activation following rating change to strong nausea (red arrow). n.b. M1 = primary motor cortex, aIns = anterior insula, amyg = amygdala.

and midcingulate cortex activation (Harrison et al. 2010). Linked activity within the anterior insula and midcingulate cortex have been postulated to integrate cognitive, affective, and interoceptive processing in order to produce behavioral and autonomic motor response (Medford and Critchley 2010). The insula and midcingulate have also been implicated in salience detection (Downar et al. 2002; Seeley et al. 2007), which relates to assigning homeostatic relevance for both internal and external sensory inputs to the brain. Hence, we can further speculate that nausea, which is a multidimensional perceptual state, emerges from activation in a broad brain network including salience processing brain regions, in order to alert the suffering individual to important changes in interoceptive signaling, so that appropriate autonomic/motor response can be enacted.

Increasing sustained activation common to affective/emotional circuitries was also noted in pgACC, OFC, NAcc, and VTA. These structures likely support the aversive nature of nausea, and the OFC in particular may attribute hedonic valence to interoceptive afference (Elliott et al. 2010). The pgACC is an important subregion of the ACC that is also strongly related to emotion (Bush et al. 2000; Vogt 2005). The

nucleus accumbens receives mesostriatal dopaminergic modulatory input from the VTA, as well as inputs from both limbic and prefrontal cortical regions. It has most commonly been linked with both aversion and reward circuitries (Carlezon and Thomas 2009).

Brain activity in bilateral prefrontal cortical regions (dlPFC) demonstrated sustained postrating activation with increasing nausea levels. The frontal gyrus was previously implicated in nausea using magnetoencephalography (Miller et al. 1996), and these prefrontal cortical regions may support the cognitive/evaluative disruption noted in our SSQ results (Lacount et al. 2009). Future studies should explicitly investigate the role that these regions play in how nausea modulates cognition/attention and vice versa (Koch 1999).

Both SI and SII also demonstrated sustained postrating activation with increasing nausea sensation. This result is notable, as our visual experimental stimulation did not involve any somatosensory afference; in contrast to visceral balloon inflation studies, which also elicit activation in both interoceptive and somatosensory brain regions (Mayer et al. 2009). In our data, SI activity was localized to a somatotopic location (ventrolateral subregion of the postcentral gyrus) consistent with the upper GI cortical representation reported in animals (Bruggemann et al. 1997) and humans (Coen et al. 2007; Van Oudenhove et al. 2008). Interestingly, lesion studies suggest that somatosensory cortices may also support interoception (Khalsa et al. 2009), and for nausea, may relate to cues from mechanoreceptors overlying the epigastrium (e.g., gastric tachyarrhythmia is increased during nausea, Hu et al. 1999).

The physiological mechanism underlying motion sickness is postulated to be visual–vestibular conflict (Bles et al. 2000). Our data demonstrated robust attention (SPL, premotor) and striate as well as extrastriate (V1 and MT+/V5, respectively) activation to translating stripes visual stimulation for all subjects. Previous neuroimaging studies of apparent self-motion using both stationary (Riedel et al. 2005) and translating (Brandt et al. 1998) visual stimuli also suggested that vection is mediated by activity in MT+/V5 and parietooccipital visual areas. However, these studies explicitly avoided or did not report motion sickness response. In our study, neither visual structures nor brainstem vestibular nuclei were parametrically activated with increasing nausea; hence, we believe that the brain response reported is indeed specific to nausea perception and not visual/vestibular integration per se.

Future studies should extend our approach to investigate disease states associated with nausea, such as cyclic vomiting syndrome (Olden and Chepyala 2008), and migraine (Cuomo-Granston and Drummond 2010), as well as the central effects of both pharmacological (e.g., dronabinol, scopolamine) and nonpharmacological (e.g., acupuncture) interventions known to modulate nausea perception. Additionally, the brain circuitry supporting cardiovagal modulation by nausea should be investigated, as autonomic outflow is an important aspect of nausea perception, and our previous study (Lacount et al. 2011) suggested that both phasic and sustained sympathovagal balance is disrupted in our motion sickness model.

Due to limitations in recruitment, our results can only generalize to females experiencing nausea from motion sickness. While gender weakly affects motion sickness susceptibility (Klosterhalfen et al. 2006), future studies should directly recruit male subjects. Finally, we found no results in several medullary (e.g., nucleus tractus solitarius and area postrema) or cerebellar

(flocculus, vermis) nuclei implicated in rat models (Horn et al. 2007). On the one hand, recent lesion studies in rats suggest that the vestibular cerebellum is not essential in the development of motion sickness (Uno et al. 2000). Conversely, medullary nuclei are at the limit of fMRI spatial resolution, and signals from these regions are plagued by cardiorespiratory artifacts. Future studies should apply methods specific to brainstem neuroimaging in order to better evaluate contributions of other brainstem nuclei than those found by our analysis.

In conclusion, fMRI can successfully be applied to evaluate different aspects of the temporal evolution of nausea. While increasing fear signaling involving noradrenergic brainstem regions may precipitate strong nausea, sustained activation following strong nausea occurs in a broader network of interoceptive, limbic, somatosensory, and cognitive processing brain areas. Identifying potential brain mechanisms underlying nausea will allow future research to target therapeutics for this aversive commonly occurring symptom.

References

Andersson M, Jenkinson, Smith S. 2007. Non-linear optimisation. FMRIB Technical Report TR07JA1. Available from: URL http://www.fmrib.ox.ac.uk/analysis/techrep.

Beckmann CF, Jenkinson M, Smith SM. 2003. General multilevel linear modeling for group analysis in fMRI. Neuroimage. 20(2): 1052–1063.

Beckmann CF, Smith SM. 2004. Probabilistic independent component analysis for functional magnetic resonance imaging. IEEE Trans Med Imaging. 23(2):137–152.

Benarroch EE. 2009. The locus ceruleus norepinephrine system: functional organization and potential clinical significance. Neurology. 73(20):1699–1704.

Bles W, Bos JE, Kruit H. 2000. Motion sickness. Curr Opin Neurol. 13(1):19–25.

Brandt T, Bartenstein P, Janek A, Dieterich M. 1998. Reciprocal inhibitory visual-vestibular interaction. Visual motion stimulation deactivates the parieto-insular vestibular cortex. Brain J Neurol. 121(Pt 9):1749–1758.

Bruggemann J, Shi T, Apkarian AV. 1997. Viscero-somatic neurons in the primary somatosensory cortex (SI) of the squirrel monkey. Brain Res. 756(1–2):297–300.

Bush G, Luu P, Posner MI. 2000. Cognitive and emotional influences in anterior cingulate cortex. Trends Cogn Sci. 4(6):215–222.

Cameron OG. 2001. Interoception: the inside story—a model for psychosomatic processes. Psychosom Med. 63(5):697–710.

Carlezon WA Jr, Thomas MJ. 2009. Biological substrates of reward and aversion: a nucleus accumbens activity hypothesis. Neuropharmacology. 56(Suppl 1):122–132.

Coen SJ, Gregory LJ, Yaguez L, Amaro E Jr, Brammer M, Williams SC, Aziz Q. 2007. Reproducibility of human brain activity evoked by esophageal stimulation using functional magnetic resonance imaging. Am J Physiol Gastrointest Liver Physiol. 293(1):G188–G197.

Cox RW. 1996. AFNI: software for analysis and visualization of functional magnetic resonance neuroimages. Comput Biomed Res. 29(3):162–173.

Craig AD. 2002. How do you feel? Interoception: the sense of the physiological condition of the body. Nat Rev Neurosci. 3(8):655–666.

Critchley HD, Wiens S, Rotshtein P, Ohman A, Dolan RJ. 2004. Neural systems supporting interoceptive awareness. Nat Neurosci. 7(2):189–195.

Cuomo-Granston A, Drummond PD. 2010. Migraine and motion sickness: what is the link? Prog Neurobiol. 91(4):300–312.

Downar J, Crawley AP, Mikulis DJ, Davis KD. 2002. A cortical network sensitive to stimulus salience in a neutral behavioral context across multiple sensory modalities. J Neurophysiol. 87(1):615–620.

Dworkin BR. 2007. Interoception. In: Cacciopo JT, Tassinary LG, Bernston GG, editors. Handbook of psychophysiology. Cambridge: Cambridge University Press. p. 482–506.

Elliott R, Agnew Z, Deakin JF. 2010. Hedonic and informational functions of the human orbitofrontal cortex. Cereb Cortex. 20(1):198–204.

Golding JF. 1998. Motion sickness susceptibility questionnaire revised and its relationship to other forms of sickness. Brain Res Bull. 47(5):507–516.

Graybiel AM. 2005. The basal ganglia: learning new tricks and loving it. Curr Opin Neurobiol. 15(6):638–644.

Harrison NA, Gray MA, Gianaros PJ, Critchley HD. 2010. The embodiment of emotional feelings in the brain. J Neurosci. 30(38):12878–12884.

Horn CC. 2008. Why is the neurobiology of nausea and vomiting so important? Appetite. 50(2–3):430–434.

Horn CC, Ciucci M, Chaudhury A. 2007. Brain Fos expression during 48 h after cisplatin treatment: neural pathways for acute and delayed visceral sickness. Auton Neurosci. 132(1–2):44–51.

Hu S, Mcchesney KA, Player KA, Bahl AM, Buchanan JB, Scozzafava JE. 1999. Systematic investigation of physiological correlates of motion sickness induced by viewing an optokinetic rotating drum. Aviat Space Environ Med. 70(8):759–765.

Kennedy RS, Berbaum KS, Lilienthal MG, Smith MG. 1993. Disorientation and natural disequilibrium from simulated flight. Int Symp Aviat Psychol. 7(26–29):799–804.

Kennedy RS, Drexler J, Kennedy RC. 2010. Research in visually induced motion sickness. Appl Ergon. 41(4):494–503.

Khalsa SS, Rudrauf D, Feinstein JS, Tranel D. 2009. The pathways of interoceptive awareness. Nat Neurosci. 12(12):1494–1496.

Klosterhalfen S, Pan F, Kellermann S, Enck P. 2006. Gender and race as determinants of nausea induced by circular vection. Gend Med. 3(3):236–242.

Koch KL. 1999. Illusory self-motion and motion sickness: a model for brain-gut interactions and nausea. Dig Dis Sci. 44(8 Suppl):53S–57S.

Kowalski A, Rapps N, Enck P. 2006. Functional cortical imaging of nausea and vomiting: a possible approach. Auton Neurosci. 129(1–2):28–35.

Lacount L, Napadow V, Kuo B, Park K, Kim J, Brown E, Barbieri R. 2009. Dynamic cardiovagal response to motion sickness: a point-process heart rate variability study. Comput Cardiol. 36:49–52.

Lacount LT, Barbieri R, Park K, Kim J, Brown EN, Kuo B, Napadow V. 2011. Static and dynamic autonomic response with increasing nausea perception. Aviat Space Environ Med. 82(4):424–433.

Ledoux J. 2003. The emotional brain, fear, and the amygdala. Cell Mol Neurobiol. 23(4–5):727–738.

Mayer EA, Aziz Q, Coen S, Kern M, Labus JS, Lane R, Kuo B, Naliboff B, Tracey I. 2009. Brain imaging approaches to the study of functional GI disorders: a Rome working team report. Neurogastroenterol Motil. 21(6):579–596.

Medford N, Critchley HD. 2010. Conjoint activity of anterior insular and anterior cingulate cortex: awareness and response. Brain Struct Funct. 214(5-6):535-549.

Miller AD, Rowley HA, Roberts TP, Kucharczyk J. 1996. Human cortical activity during vestibular- and drug-induced nausea detected using MSI. Ann N Y Acad Sci. 781:670-672.

Morrow GR, Andrews PL, Hickok JT, Stern R. 2000. Vagal changes following cancer chemotherapy: implications for the development of nausea. Psychophysiology. 37(3):378-384.

Muth ER, Stern RM, Thayer JF, Koch KL. 1996. Assessment of the multiple dimensions of nausea: the Nausea Profile (NP). J Psychosom Res. 40(5):511-520.

Olden KW, Chepyala P. 2008. Functional nausea and vomiting. Nat Clin Pract Gastroenterol Hepatol. 5(4):202-208.

Oldfield RC. 1971. The assessment and analysis of handedness: the Edinburgh inventory. Neuropsychologia. 9(1):97-113.

Quigley EM, Hasler WL, Parkman HP. 2001. AGA technical review on nausea and vomiting. Gastroenterology. 120(1):263-286.

Riedel E, Stephan T, Deutschlander A, Kalla R, Wiesmann M, Dieterich M, Brandt T. 2005. Imaging the visual autokinetic illusion with fMRI. Neuroimage. 27(1):163-166.

Robinson BW, Mishkin M. 1968. Alimentary responses to forebrain stimulation in monkeys. Exp Brain Res (Experimentelle Hirnforschung. Experimentation Cerebrale). 4(4):330-366.

Schenberg EE, Ferreira TL, Figueredo LZ, Hipolide DC, Nobrega JN, Oliveira MG. 2006. Fear conditioning performance and NMDA receptor subtypes: NR2A differential expression in the striatum. Brain Res Bull. 69(4):440-446.

Seeley WW, Menon V, Schatzberg AF, Keller J, Glover GH, Kenna H, Reiss AL, Greicius MD. 2007. Dissociable intrinsic connectivity networks for salience processing and executive control. J Neurosci. 27(9):2349-2356.

Stern R, Koch K, Andrews P. 2011. Nausea: mechanisms and management. New York: Oxford University Press.

Uno A, Takeda N, Kitahara T, Sakata Y, Yamatodani A, Kubo T. 2000. Effects of vestibular and cerebellum lesion on motion sickness in rats. Acta Oto-laryngologica. 120(3):386-389.

Valentino RJ, Curtis AL, Page ME, Pavcovich LA, Florin-Lechner SM. 1998. Activation of the locus ceruleus brain noradrenergic system during stress: circuitry, consequences, and regulation. Adv Pharmacol. 42:781-784.

Van Oudenhove L, Dupont P, Vandenberghe J, Geeraerts B, Van Laere K, Bormans G, Demyttenaere K, Tack J. 2008. The role of somatosensory cortical regions in the processing of painful gastric fundic distension: an update of brain imaging findings. Neurogastroenterol Motil. 20(5):479-487.

Vogt BA. 2005. Pain and emotion interactions in subregions of the cingulate gyrus. Nat Rev Neurosci. 6(7):533-544.

Wiens S. 2005. Interoception in emotional experience. Curr Opin Neurol. 18(4):442-447.

Wiggins GC, Triantafyllou C, Potthast A, Reykowski A, Nittka M, Wald LL. 2006. 32-channel 3 Tesla receive-only phased-array head coil with soccer-ball element geometry. Magn Reson Med. 56(1):216-223.

Yen Pik Sang FD, Golding JF, Gresty MA. 2003. Suppression of sickness by controlled breathing during mildly nauseogenic motion. Aviat Space Environ Med. 74(9):998-1002.